Integrated hollow-core fibers for nonlinear optofluidic applications

Limin Xiao,* Natalie V. Wheeler, Noel Healy, and Anna C. Peacock

Optoelectronics Research Centre, University of Southampton, Southampton SO17 1BJ, UK
*lx1v10@orc.soton.ac.uk

Abstract: A method to fabricate all-in-fiber liquid microcells has been demonstrated which allows for the incorporation of complex hollow-core photonic crystal fibers (HCPCFs). The approach is based on a mechanical splicing method in which the hollow-core fibers are pigtailed with telecoms fibers to yield devices that have low insertion losses, are highly compact, and do not suffer from evaporation of the core material. To isolate the PCF cores for the infiltration of low index liquids, a pulsed CO_2 laser cleaving technique has been developed which seals only the very ends of the cladding holes, thus minimizing degradation of the guiding properties at the coupling region. The efficiency of this integration method has been verified via strong cascaded Raman scattering in both toluene (high index) core capillaries and ethanol (low index) core HCPCFs, for power thresholds up to six orders of magnitude lower than previous results. We anticipate that this stable, robust all-fiber integration approach will open up new possibilities for the exploration of optofluidic interactions.

OCIS codes: (060.2340) Fiber optics components; (060.5295) Photonic crystal fibers; (060.4370) Nonlinear optics, fibers.

References and links

1. F. Benabid, F. Couny, J. C. Knight, T. A. Birks, and P. St. J. Russell, "Compact, stable and efficient all-fibre gas cells using hollow-core photonic crystal fibres," Nature **434**(7032), 488–491 (2005).
2. M. Vieweg, T. Gissibl, S. Pricking, B. T. Kuhlmey, D. C. Wu, B. J. Eggleton, and H. Giessen, "Ultrafast nonlinear optofluidics in selectively liquid-filled photonic crystal fibers," Opt. Express **18**(24), 25232–25240 (2010).
3. C. de Matos, L. de S. Menezes, A. Brito-Silva, M. Martinez Gámez, A. Gomes, and C. de Araújo, "Random fiber laser," Phys. Rev. Lett. **99**(15), 153903 (2007).
4. H. W. Lee, M. A. Schmidt, and P. St. J. Russell, "Excitation of a nanowire "molecule" in gold-filled photonic crystal fiber," Opt. Lett. **37**(14), 2946–2948 (2012).
5. C.-H. Lee, C.-H. Chen, C.-L. Kao, C.-P. Yu, S.-M. Yeh, W.-H. Cheng, and T.-H. Lin, "Photo and electrical tunable effects in photonic liquid crystal fiber," Opt. Express **18**(3), 2814–2821 (2010).
6. C. P. Yu and J. H. Liou, "Selectively liquid-filled photonic crystal fibers for optical devices," Opt. Express **17**(11), 8729–8734 (2009).
7. Y. Han, S. Tan, M. K. Oo, D. Pristinski, S. Sukhishvili, and H. Du, "Towards full-length accumulative surface-enhanced Raman scattering-active photonic crystal fibers," Adv. Mater. **22**(24), 2647–2651 (2010).
8. S. Unterkofler, R. J. McQuitty, T. G. Euser, N. J. Farrer, P. J. Sadler, and P. St. J. Russell, "Microfluidic integration of photonic crystal fibers for online photochemical reaction analysis," Opt. Lett. **37**(11), 1952–1954 (2012).
9. S. Yiou, P. Delaye, A. Rouvie, J. Chinaud, R. Frey, G. Roosen, P. Viale, S. Février, P. Roy, J.-L. Auguste, and J.-M. Blondy, "Stimulated Raman scattering in an ethanol core microstructured optical fiber," Opt. Express **13**(12), 4786–4791 (2005).
10. J. Bethge, A. Husakou, F. Mitschke, F. Noack, U. Griebner, G. Steinmeyer, and J. Herrmann, "Two-octave supercontinuum generation in a water-filled photonic crystal fiber," Opt. Express **18**(6), 6230–6240 (2010).
11. J. C. Travers, W. Chang, J. Nold, N. Y. Joly, and P. St. J. Russell, "Ultrafast nonlinear optics in gas-filled hollow-core photonic crystal fibers," J. Opt. Soc. Am. B **28**, A11–A26 (2011).
12. K. Kieu, L. Schneebeli, R. A. Norwood, and N. Peyghambarian, "Integrated liquid-core optical fibers for ultra-efficient nonlinear liquid photonics," Opt. Express **20**(7), 8148–8154 (2012).
13. K. Kieu, L. Schneebeli, E. Merzlyak, J. M. Hales, A. DeSimone, J. W. Perry, R. A. Norwood, and N. Peyghambarian, "All-optical switching based on inverse Raman scattering in liquid-core optical fibers," Opt. Lett. **37**(5), 942–944 (2012).

#196385 - $15.00 USD Received 26 Aug 2013; revised 8 Nov 2013; accepted 11 Nov 2013; published 14 Nov 2013

14. J. S. K. Ong, T. Facincani, and C. J. S. de Matos, "Evaporation in water-core photonic crystal fibers," Proc. AIP Conf. **152** (2008).
15. R. M. Gerosa, A. Bozolan, C. J. S. de Matos, M. A. Romero, and C. M. B. Cordeiro, "Novel sealing technique for practical liquid-core photonic crystal fibers," IEEE Photon. Technol. Lett. **24**(3), 191–193 (2012).
16. J. Park, J. Kim, B. Paulson, and K. Oh, "Liquid core photonic crystal fiber with the enhanced light coupling efficiency," in Proceedings of the IEEE IPC Photonics Conference (IEEE, 2012), pp. 808–809.
17. S. Kedenburg, M. Vieweg, T. Gissibl, and H. Giessen, "Linear refractive index and absorption measurements of nonlinear optical liquids in the visible and near-infrared spectral region," Opt. Mater. Express **2**(11), 1588–1611 (2012).
18. C. Conti, M. A. Schmidt, P. St. J. Russell, and F. Biancalana, "Highly noninstantaneous solitons in liquid-core photonic crystal fibers," Phys. Rev. Lett. **105**(26), 263902 (2010).
19. D. Lopez-Cortes, O. Tarasenko, and W. Margulis, "All-fiber Kerr cell," Opt. Lett. **37**(15), 3288–3290 (2012).
20. L. Xiao, W. Jin, M. Demokan, H. Ho, Y. Hoo, and C. Zhao, "Fabrication of selective injection microstructured optical fibers with a conventional fusion splicer," Opt. Express **13**(22), 9014–9022 (2005).
21. K. Nielsen, D. Noordegraaf, T. Sørensen, A. Bjarklev, and T. P. Hansen, "Selective filling of photonic crystal fibres," J. Opt. A, Pure Appl. Opt. **7**(8), L13–L20 (2005).
22. F. F. Dai, Y. H. Xu, and X. F. Chen, "Enhanced and broadened SRS spectra of toluene mixed with chloroform in liquid-core fiber," Opt. Express **17**(22), 19882–19886 (2009).

1. Introduction

All-in-fiber microcells provide a useful platform from which to investigate the interaction between light and fluidic media [1–5]. Compared to the traditional bulk gas cells and liquid cuvettes, fibers with hollow micro-scale cores can provide high intensities over much longer interaction lengths. As such, they can facilitate strong light-fluid interactions that are highly desirable for the development of efficient laser devices [1–6], optofluidic sensors [7, 8], and nonlinear optical applications [9–13]. Furthermore, by integrating the microcells with telecoms fibers there is potential to exploit material properties that are unique to fluids in a compact and stable geometry for application in wide ranging areas. For example, gas fiber microcells made from hollow-core photonic crystal fibers (HCPCFs) have found use in compact gas lasers, laser frequency locking, and high-harmonic generation [1, 11], while liquid fiber microcells have been demonstrated for wavelength conversion and high-speed optical switching [2, 13]. However, although it is relatively straightforward to splice the gas cells directly to telecoms fibers, even for highly flammable gases [1], in general integrated liquid cells are much more complicated to fabricate as any air bubbles inside the liquid or at the joint interfaces will cause significant propagation losses [14–16]. As a result, integrated liquid cells have to date been restricted to the use of simple capillary fibers (CFs) so that the fluid index must be higher than that of silica in order for the core to guide via total internal reflection (TIR). The ability to integrate HCPCFs into a liquid microcell would thus be highly advantageous in terms of extending the range of accessible liquids [17], though would also allow for extensive tailoring of the dispersion and nonlinear properties through design of the microstructured cladding. This latter point is of significant interest for investigating both the temporal and spatial dynamics of nonlinear phenomena such as solitons in microfluidic waveguides [2,18].

Previous approaches to integrating liquid microcells with telecoms fibers have typically employed fusion splicing methods. Kieu *et al.* [12, 13] have developed a gap-splicing method, where the liquid is infiltrated through a glass vial positioned over the join. This approach allows for low-loss integration, though the use of a bulky liquid container negates many of the fiber benefits such as compactness and flexibility. Alternatively, Lopez-Cortes *et al.* [19] have utilized a multiple splicing method to allow liquid to flow through various multi-hole CFs resulting in a device that is completely fiberized and highly compact, though somewhat complex to fabricate. Whether either of these methods could be used for the construction of microcells with complex HCPCFs has yet be determined, though there are obvious challenges to overcome both in terms of optimizing the splicing and avoiding unwanted filling of the cladding holes.

Here we propose a new approach to fabricating all-in-fiber liquid microcells (AFLMs) that is compatible with a wide range of CFs and PCF platforms, and provide the first demonstration of an integrated HCPCF device. The method is based on mechanically splicing

#196385 - $15.00 USD Received 26 Aug 2013; revised 8 Nov 2013; accepted 11 Nov 2013; published 14 Nov 2013

the microcells to telecoms fibers using large diameter tapered capillaries as sleeves, which also act as containers for the liquid. The compact devices are completely sealed so that they are stable, robust, and flexible to handle. To allow for selective filling into the cores of HCPCFs, we have also developed a simple and effective method to seal the cladding holes using a pulsed CO_2 laser, which minimizes any disruption to the guiding properties at the coupling region. The suitability of this integration approach for wide ranging materials investigations is demonstrated through efficient cascaded Raman scattering both in high index (toluene) core CFs and low index (ethanol) core HCPCFs.

2. Principle and experiments

Complete integration of liquid microcells is important not only to improve the handleability of devices, but also to avoid liquid evaporation for stable operation. The basic idea of our mechanical splicing method is illustrated in Fig. 1. The process starts with each end of the fiber microcell being inserted into a wide diameter (~150 μm internal diameter) capillary sleeve. To aid with the alignment, the sleeves are tapered to have a waist with an inner diameter equal to the outer diameter of standard fibers (~125 μm). The choice of taper waist also ensures that the sleeved fibers are held tightly so that they are less susceptible to misalignment when moved. The liquid is then infiltrated into the microcell either via capillary action or through pumping with a syringe until it is completely filled. The tapered sleeve can also be used to hold extra liquid, so that if any evaporation does occur the core remains fully filled and the coupling facets are not compromised. Finally, two single mode fibers (SMFs) are inserted into the open ends of the sleeves to form the seamless joints. Care should be taken during the insertion so that any trapped air at the endface of the SMF can leak out through the liquid filled gap between the SMF and sleeve. The ends of the sleeves are then sealed using a suitable adhesive to improve the device stability.

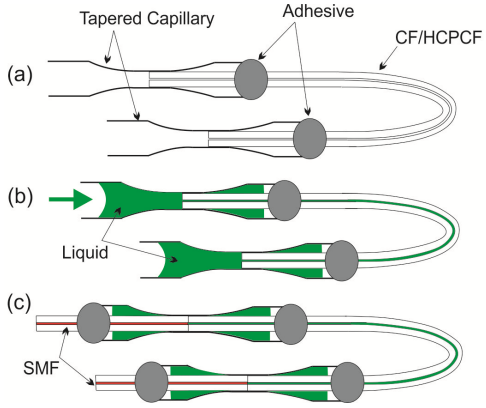

Fig. 1. Schematic of AFLM fabrication. (a) A CF/HCPCF is inserted into tapered capillary sleeves. (b) Liquid is pumped into the fiber core, with the ends immersed in excess volume to avoid evaporation. (c) SMFs are carefully inserted into the sleeves and mechanically spliced to the liquid-core fiber.

Figure 2 shows the experimental setup to make a AFLM using a standard CF. The sleeved CF and syringe needle were pushed through a polymer septum of a cap into a vial filled with toluene, see Fig. 2(a), which has an index of n~1.50 at 532 nm (>n_{silica}~1.46). The syringe was connected to a controllable pressure cylinder to force the liquid through the CF, with a typical applied pressure of ~1-2 bar. Figure 2(b) shows the other end of the CF inserted inside the tapered sleeve, which has an outer diameter of ~335 μm (tapered down from 400 μm). The complete filling of the CF is confirmed in Fig. 2(c) where the toluene can be seen to flow into the tapered sleeve, a process that was typically completed within minutes for a few tens of centimeters, and in less than half an hour for several meters. The final stage in Fig. 2(d) shows the inserted Corning SMF-28 fiber aligned to the liquid-core CF, from which it can be seen that there is no trapped air at the interface joint. To illustrate some of the advantages of

#196385 - $15.00 USD Received 26 Aug 2013; revised 8 Nov 2013; accepted 11 Nov 2013; published 14 Nov 2013

this method, Figs. 2(e) and 2(f) show a comparison between an AFLM device and that of the gap-splicing approach [12]. It is clear that the AFLM in Fig. 2(f) is not only more compact, but is also easier to handle and can be moved around without any additional stabilization (such as the microscope slide in Fig. 2(e)). Furthermore, the robustness of the AFLM could be improved, for example, by inserting into a steel tube protector.

To investigate the insertion losses associated with the AFLM devices, transmission measurements were conducted on two CFs, both 0.5 m in length, but with different inner core diameters of 10 µm and 5 µm. For the 10 µm CF we measured a device transmission of up to 80% at a wavelength of 690 nm, where the toluene loss is ~0.4 dB/m (~5% loss due to material) [17]. As the mismatch between the fundamental fiber modes is very low (<0.05 dB as calculated via the overlap integrals), we attribute the remaining loss to scattering and some minimal interface loss. For the 5 µm CF the device transmission is reduced to ~40%, from which we attribute the additional 2.3 dB loss to the modal mismatch between the SMF and smaller toluene core CF. It is worth noting that we can achieve a ~10% increase in the coupling efficiency when comparing our mechanical method versus that of the gap-splicing approach, as calculated for the devices shown in Fig. 2 fabricated with 5 µm core CFs.

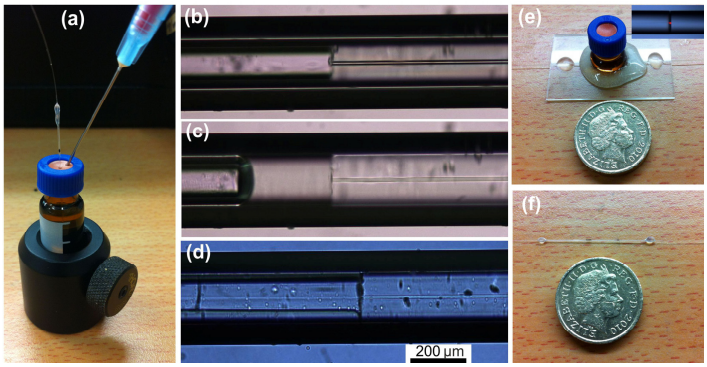

Fig. 2. (a) Photo of the filling process. (b) The CF is inserted in a tapered capillary. (c) Liquid flows through the CF until complete filling so that the endface is immersed in liquid. (d) The SMF on the left-hand side is seamlessly aligned to the toluene core CF. Photographs of (e) an integrated device using the gap-splicing method used in [12] and (f) our mechanically spliced AFLM. The inset in (e) shows light coupled through the gap-splicing joint.

Having demonstrated the practically of our mechanical splicing method for CFs, we looked to extend this to the integration of more complex HCPCFs. Although it would be straightforward to completely fill the PCFs with the liquids which, for example, would be of use for investigations of spatial or non-localized solitons [2,18], our aim for this work was to construct a device which retained the air-silica cladding structure so that the core could be used to incorporate a liquid with an index lower than silica, and yet still guide via TIR. Various methods have been developed to fill the center core of HCPCFs by blocking the cladding holes [20, 21], though these typically disrupt the guiding properties at the fiber ends so that they cannot be butt coupled to SMF. To mitigate this, we have established a new technique to seal the cladding holes using a pulsed CO_2 laser cleaver. The method makes use of the fact that when laser cleaving PCFs, a thin layer of silica melts to cover the end-face and block the holes, without inducing any longitudinal deformation. Owing to the reduced silica content near the core of a HCPCF, it is thus possible to adjust the laser parameters so that the cladding holes are covered while the large center core remains open, as illustrated via the schematic in Fig. 3(a). For the HCPCF used in our work, we found that with the optimum laser parameters of P_{peak} = 250 W, ΔT_{fwhm} = 150 µs, and a repetition rate of 1 kHz, we could cover the cladding holes with 10 incident pulses, but yet the deformation length was as short as ~14 µm, as shown in Fig. 3(b). For comparison, Fig. 3(c) shows the minimum deformation length of ~130 µm obtained when using the popular method of collapsing the cladding holes with a fusion splicer [20]. It is clear from these results that as the focused laser cleaving

#196385 - $15.00 USD Received 26 Aug 2013; revised 8 Nov 2013; accepted 11 Nov 2013; published 14 Nov 2013

method reduces the heat zone, this greatly minimizes the region over which the holes are collapsed to lessen any disruption to guided light, allowing for butt coupling to SMF.

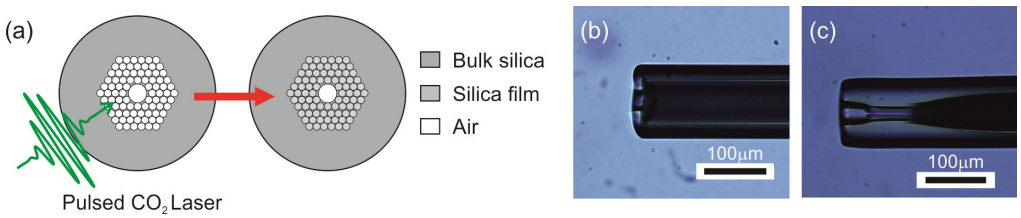

Fig. 3. (a) Schematic of the pulsed CO_2 laser cleaving method. (b) Microscope image showing longitudinal deformation of the HCPCF when the cladding holes are blocked via the CO_2 laser cleaving method. (c) Holes blocked a fusion splicing method for comparison [20].

Figure 4(a) shows the cross-sectional image of the HCPCF from Fig. 3(b) before the cladding holes were sealed. This HCPCF was not specifically designed for coupling to an SMF and had a large core diameter of ~23 μm, as well as a large 165 μm outer cladding that had to be tapered down to 125 μm at the ends to fit into the sleeve (~18.7 μm core diameter), though this could be done with minimal impact to the microstructure (see inset). The cross-section of the laser processed HCPCF is shown in Fig. 4(b), from which it can be seen that although all of the cladding holes are closed, the center hole has remained open with only a slight shrinkage of ~6% (17.6 μm core). Integration of the HCPCF with the SMF pigtails then follows the same procedure as Fig. 2, with the fabricated device shown in Fig. 4(c). Owing to the low index (air-silica) cladding, the HCPCF core could be filled with low index ethanol, n~1.36 at 532 nm, as illustrated in Fig. 4(d). The measured device transmission for a 0.5 m long HCPCF-AFLM at 635 nm was ~50%, where the ethanol loss is 1 dB/m (~10% material loss) [17]. We attribute the remaining loss to a combination of the mode mismatch (~1 dB), tapering losses (~0.5 dB), as well as some scattering and minimal interface loss as before. Owing to the large core size, it is also quite likely that coupling into high order modes may occur, which will reduce the efficiency of the light-fluid interactions. Nevertheless, the fabricated device serves to demonstrate the proof-of-concept for integrated HCPCFs, and the transmission of this device is still much higher than in previous investigations of non-integrated HCPCFs [10] due to the improved stability of the coupling facet. We expect that the overall transmission and efficiency of the PCF-AFLM devices would be improved significantly with a specially designed HCPCF, which is subject to ongoing research.

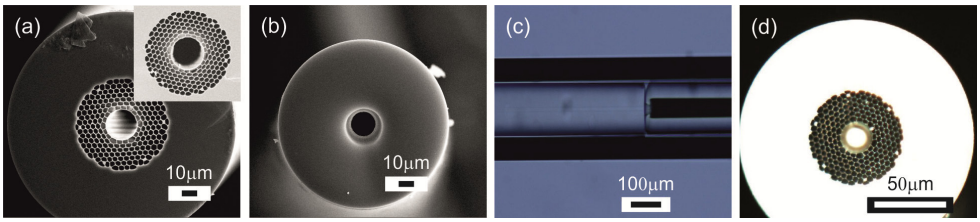

Fig. 4. (a) Scanning electron micrograph (SEM) of the HCPCF (inset: tapered end on same scale). (b) SEM of cross-section after sealing the cladding holes with the CO_2 laser (c) Microscope image of the integrated SMF seamlessly aligned to the ethanol core HCPCF. (d) Microscopic end view of ethanol core HCPCF.

To investigate the efficiency of our mechanical splicing approach for nonlinear light-fluid interactions, we use the set-up in Fig. 5(a) to measure the stimulated Raman scattering (SRS) spectra from the AFLM devices. The pump laser is a frequency doubled Nd:YVO_4 Q-switched 10 ns pulsed source at 532 nm, with a repetition rate of 20 Hz. A short pass wavelength filter was used to remove the residual 1064 nm pump before launching into the fiber system and the input power was adjusted using a tunable attenuator. The SRS spectrum obtained for the 0.5 m long toluene filled 5 μm core CF-AFLM is shown in Fig. 5(b), at an average pump power of 30 μW (150 W peak power). We note that the threshold of the first

#196385 - $15.00 USD Received 26 Aug 2013; revised 8 Nov 2013; accepted 11 Nov 2013; published 14 Nov 2013

stokes line is only 8.5 μW (peak power of 42.5 W), which compared to previous reports is around 6 orders of magnitude lower [22]. We attribute this greatly improved efficiency both to the lower device insertion loss of our all-fiber system and its compatibility with small core capillaries (a reduction of ten times over the core size in [22]). Careful inspection of the spectrum reveals that as well as the four cascaded stokes lines corresponding to the aromatic ring mode at a shift of 1006 cm^{-1} (562 nm, 596 nm, 634 nm, and 677 nm), it is also possible to identify the first stokes of the CH stretching mode at 3060 cm^{-1} (636 nm). Furthermore, from the inset we can see that the strong aromatic stokes line at 562nm is also able to pump the CH stretch, as evidenced by the second peak at 679 nm. Thus the high efficiency of this device demonstrates the potential for these AFLMs to find use in investigations of more complex, multi-stage light-fluid interactions.

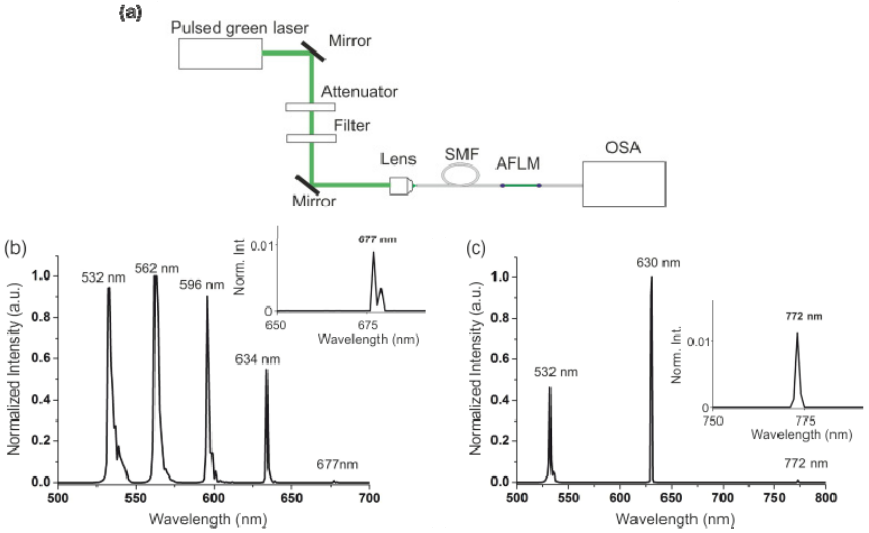

Fig. 5. (a) Experimental setup for SRS. (b) Cascaded Raman spectrum of a toluene core CF-AFLM. (c) Cascaded Raman spectrum of ethanol core HCPCF-AFLM.

Finally, Fig. 5(c) shows the SRS spectrum obtained for the ethanol HCPCF-AFLM. In this experiment a longer 2.5 m device was used to extend the interaction length owing to the use of the large core HCPCF (~23 μm), which was similar to the 2.8 m length used by Yiou *et al.* in [9] for an 11 μm core device . However, despite the larger core, we have still observed two cascaded stokes lines due to the CH stretch 2928 cm^{-1} (630 nm and 772 nm) for a coupled average power of only 54 μW (270 W peak power), i.e., a threshold three times lower than previously reported [9]. It is worth noting that the low power of the second stokes, and hence the suppression of any higher order lines, is due to the increased losses of ethanol at the longer wavelengths. Nevertheless, we anticipate that with an appropriately designed smaller core HCPCF, and a wide transparency core material, our results could be improved significantly for the observation of rich nonlinear phenomena in HCPCF-AFLMs.

3. Conclusion

In conclusion, we have demonstrated a novel approach to fabricating AFLMs which is compatible with wide ranging capillary fibers and PCFs. This integration method has the benefits of ultrahigh compactness, SMF pigtailing, and high efficiency. By combining this with a new CO_2 laser cleaving technique to selectively fill the core of a HCPCF, we can extend the liquids that can be investigated in AFLMs to cover the full complement of material indices. By exploiting the two dimension design space of the PCF cross-sections, we anticipate that our new approach will expand the exploration space of optofluidic interactions in all-in-fiber based devices.

#196385 - $15.00 USD Received 26 Aug 2013; revised 8 Nov 2013; accepted 11 Nov 2013; published 14 Nov 2013

Acknowledgments

The authors thank S. Mailis, J. Daniel, J. Hayes, J. Nilsson, N. Vukovic, P. Sazio, N. Baddela, M. Petrovich and P. Lagoudakis for equipment support. This work is funded by the UK Engineering and Physical Sciences Research Council (EP/J004863/1).

#196385 - $15.00 USD Received 26 Aug 2013; revised 8 Nov 2013; accepted 11 Nov 2013; published 14 Nov 2013